Biochemical Engineering Journal 177 (2022) 108238

Contents lists available at ScienceDirect

Biochemical Engineering Journal

journal homepage: www.elsevier.com/locate/bej

Semi-rational evolution of pyruvate carboxylase from *Rhizopus oryzae* for elevated fumaric acid synthesis in *Saccharomyces cerevisiae*

Guoqiang Xu [a,b,d,*], Xiangliu Shi [a,b,d], Yuhao Gao [a,b,d], Jiyue Wang [a,b,d], Hui Cheng [a,b,d], Yang Liu [a,b,d], Yuanyuan Chen [a,b,d], Jiayu Li [a,b,d], Xiaopeng Xu [a,b,d], Jian Zha [f], Ke Xia [e], Robert J. Linhardt [e], Xiaomei Zhang [c], Jinsong Shi [c], Mattheos A.G. Koffas [e,**], Zhenghong Xu [a,b,d,*]

[a] The Key Laboratory of Industrial Biotechnology, Ministry of Education, Jiangnan University, Wuxi 214122, China
[b] National Engineering Laboratory for Cereal Fermentation Technology, Jiangnan University, Wuxi 214122, China
[c] Laboratory of Pharmaceutical Engineering, School of Pharmaceutics, Jiangnan University, Wuxi 214122, China
[d] Jiangsu Provincial Research Center for Bioactive Product Processing Technology, Jiangnan University, Wuxi 214122, China
[e] Center for Biotechnology and Interdisciplinary Studies, and Department of Chemical and Biological Engineering, Rensselaer Polytechnic Institute, Troy, NY 12180, United States
[f] School of Food and Biological Engineering, Shaanxi University of Science and Technology, Xi'an, Shaanxi 710021, China

ARTICLE INFO

Keywords:
Semi-rational evolution
Saccharomyces cerevisiae
Fumaric acid
Pyruvate carboxylase

ABSTRACT

Dicarboxylic acids are widely used in food, pharmaceutical, and chemical industries. Pyruvate carboxylase (PYC) plays a pivotal role in the production of dicarboxylic acids in microbial fermentation process. Our previous work showed that heterologous expression of pyruvate carboxylase (*Ro*PYC) from *Rhizopus oryzae* resulted in an increase in fumaric acid titer to 226.0 ± 2.2 mg/L from 194.0 ± 4.0 mg/L in the *S. cerevisiae pdc1adh1fum1* strain. However, PYC still remained the metabolic step limiting the production of target carboxylic acids. In this study, semi-rational evolution of pyruvate carboxylase by site-saturation mutagenesis combined with codon optimization was conducted to further improve fumaric acid synthesis. We demonstrated that each of three mutations (N315F, R485P and N1078F) or codon optimization of *Ro*PYC significantly increased the production of fumaric acid. A maximal titer of 465.5 ± 6.5 mg/L was achieved in flasks by the strain expressing codon-optimized *Ro*PYC mutant (R485P). Enzyme assays of these mutants showed higher PYC activities, while homology modeling indicated that the increased PYC activities could be attributed to the modulation of the allosteric domain and the biotin carboxylation domain. In addition, both calcium ion and carbon dioxide displayed positive effects on the fumaric acid production by this mutant. Overall, the strategy described here demonstrated an effective way for elevating PYC activity and further enhance the synthesis of dicarboxylic acids.

1. Introduction

Dicarboxylic acids including malic acid, fumaric acid, succinic acid and α-ketoglutaric acid are broadly applied in food, pharmaceutical, and chemical industries [1–3]. In recent years, microbial production of these products from renewable biomass has attracted considerable interest [4]. The baking yeast, *Saccharomyces cerevisiae,* is one of the most commonly used microorganisms in biofermentative production of carboxylic acids such as fumaric acid [5]. One of the challenges in metabolic engineering for the production of dicarboxylic acids by *S. cerevisiae* involves linking the glycolytic pathway (EMP) to the synthetic pathways of target dicarboxylic acids [6]. One way to address this challenge is overexpression of pyruvate carboxylase, which plays a pivotal role in linking the EMP pathway to the synthetic pathways of target dicarboxylic acids [7–9]. However, this method commonly results in limited elevation of target dicarboxylic acids. To overcome these obstacles, site-saturation mutagenesis and codon usage optimization can be used to semi-rational evolve pyruvate carboxylase for further elevating production of dicarboxylic acids. The critical aspect of site-saturation mutagenesis is identifying the sites that should be mutated.

* Corresponding authors at: The Key Laboratory of Industrial Biotechnology, Ministry of Education, Jiangnan University, Wuxi 214122, China
** Corresponding author.
E-mail addresses: xuguoqiang@jiangnan.edu.cn (G. Xu), koffam@rpi.edu (M.A.G. Koffas), zhenghxu@jiangnan.edu.cn (Z. Xu).

https://doi.org/10.1016/j.bej.2021.108238
Received 8 July 2021; Received in revised form 29 September 2021; Accepted 11 October 2021
Available online 19 October 2021

Table 1
Strains and plasmids used in this study.

Strain or plasmid	Relevant genotype and characteristics	Source or reference
S. cerevisiae CEN. PK2–1C	*MATa;ura3–52 trp1–289 leu2–3 his3 MAL2–8C*	EUROSCARF
pdc1adh1	CEN.PK2–1C *pdc1*:: loxP *adh1*:: loxP	[10]
pdc1adh1fum1	CEN.PK2–1C *pdc1*:: loxP *adh1*:: loxP *fum1*:: loxP	[10]
pdc1adh1fum1 ↑*Ro*PYC	CEN.PK2–1C *pdc1*:: loxP *adh1*:: loxP *fum1*:: loxP pY15TEF1- *Ro*PYC	[10]
pdc1adh1fum1 ↑*Ro*PYC P474N	CEN.PK2–1C *pdc1*:: loxP *adh1*:: loxP *fum1*:: loxP pY15TEF1- *Ro*PYCP474N	[10]
pdc1adh1fum1 ↑*Ro*PYC E300C	CEN.PK2–1C *pdc1*:: loxP *adh1*:: loxP *fum1*:: loxP pY15TEF1- *Ro*PYC E300C	This work
pdc1adh1fum1 ↑*Ro*PYC N315F	CEN.PK2–1C *pdc1*:: loxP *adh1*:: loxP *fum1*:: loxP pY15TEF1- *Ro*PYC N315F	This work
pdc1adh1fum1 ↑*Ro*PYC R485P	CEN.PK2–1C *pdc1*:: loxP *adh1*:: loxP *fum1*:: loxP pY15TEF1- *Ro*PYC R485P	This work
pdc1adh1fum1 ↑*Ro*PYC N1078F	CEN.PK2–1C *pdc1*:: loxP *adh1*:: loxP *fum1*:: loxP pY15TEF1- *Ro*PYC N1078F	This work
pdc1adh1fum1 ↑*Ro*PYC N315F/ R485P	CEN.PK2–1C *pdc1*:: loxP *adh1*:: loxP *fum1*:: loxP pY15TEF1- *Ro*PYC N315F/R485P	This work
pdc1adh1fum1 ↑*Ro*PYC R485P/ N1078F	CEN.PK2–1C *pdc1*:: loxP *adh1*:: loxP *fum1*:: loxP pY15TEF1- *Ro*PYC R485P/N1078F	This work
pdc1adh1fum1 ↑*Ro*PYC N315F/ N1078F	CEN.PK2–1C *pdc1*:: loxP *adh1*:: loxP *fum1*:: loxP pY15TEF1- *Ro*PYC N315F/N1078F	This work
pdc1adh1fum1 ↑*Ro*PYC N315F/ R485P/N1078F	CEN.PK2–1C *pdc1*:: loxP *adh1*:: loxP *fum1*:: loxP pY15TEF1- *Ro*PYC N315F/R485P/ N1078F	This work
pdc1adh1fum1 ↑*Ro*PYC*	CEN.PK2–1 C *pdc1*:: loxP *adh1*:: loxP *fum1*:: loxP pY15TEF1- *Ro*PYC*	This work
pdc1adh1fum1 ↑*Ro*PYC* N315F	CEN.PK2–1 C *pdc1*:: loxP *adh1*:: loxP *fum1*:: loxP pY15TEF1- *Ro*PYC* N315F	This work
pdc1adh1fum1 ↑*Ro*PYC* R485P	CEN.PK2–1 C *pdc1*:: loxP *adh1*:: loxP *fum1*:: loxP pY15TEF1- *Ro*PYC* R485P	This work
pdc1adh1fum1 ↑*Ro*PYC* N1078F	CEN.PK2–1 C *pdc1*:: loxP *adh1*:: loxP *fum1*:: loxP pY15TEF1- *Ro*PYC* N1078F	This work
pdc1adh1fum1 ↑*Ro*PYC* N315F/ R485P	CEN.PK2–1 C *pdc1*:: loxP *adh1*:: loxP *fum1*:: loxP pY15TEF1- *Ro*PYC* N315F/R485P	This work
pdc1adh1fum1 ↑*Ro*PYC* R485P/ N1078F	CEN.PK2–1 C *pdc1*:: loxP *adh1*:: loxP *fum1*:: loxP pY15TEF1- *Ro*PYC* R485P/N1078F	This work
pdc1adh1fum1 ↑*Ro*PYC* N315F/ N1078F	CEN.PK2–1 C *pdc1*:: loxP *adh1*:: loxP *fum1*:: loxP pY15TEF1- *Ro*PYC* N315F/N1078F	This work
pdc1adh1fum1 ↑*Ro*PYC* N315F/ R485P/N1078F	CEN.PK2–1 C *pdc1*:: loxP *adh1*:: loxP *fum1*:: loxP pY15TEF1- *Ro*PYC*N315F/R485P/ N1078F	This work
pY15TEF1- *Ro*PYC	Amp, LEU2, the *Ro*PYC orf in pY15TEF1	[8]
pY15TEF1- *Ro*PYC*	Amp, LEU2, the condon optimized *Ro*PYC orf in pY15TEF1	This work
pGFP33	GFP tag and CYC1 terminator inserted into the *Sph*I and *Hind*III sites of YCplac33	Michael Hall provided
pGFP33-TEF1p-*Ro*PYC	The TEF1 promoter and *Ro*PYC orf in pGFP33	This work
pY15TEF1	Amp, LEU2	Lab collection
pY15TEF1-*Ro*PYC	Amp, LEU2, the *Ro*PYC orf in pY15TEF1	Lab collection
pY15TEF1-*Ro*PYC P474N	Amp, LEU2, the *Ro*PYCP474N orf in pY15TEF1	This work
pY15TEF1-*Ro*PYC E300C	Amp, LEU2, the *Ro*PYC E300C orf in pY15TEF1	This work
pY15TEF1-*Ro*PYC N315F	Amp, LEU2, the *Ro*PYC N315F orf in pY15TEF1	This work
pY15TEF1-*Ro*PYC R485P	Amp, LEU2, the *Ro*PYC R485P orf in pY15TEF1	This work
pY15TEF1-*Ro*PYC N1078F	Amp, LEU2, the *Ro*PYC N1078F orf in pY15TEF1	This work
pY15TEF1-*Ro*PYC N315F/R485P	Amp, LEU2, the *Ro*PYC N315F/ R485P orf in pY15TEF1	This work
pY15TEF1-*Ro*PYC R485P/N1078F	Amp, LEU2, the *Ro*PYC R485P/ N1078F orf in pY15TEF1	This work
pY15TEF1-*Ro*PYC N315F/N1078F	Amp, LEU2, the *Ro*PYC N315F/ N1078F orf in pY15TEF1	This work
pY15TEF1-*Ro*PYC N315F/R485P/ N1078F	Amp, LEU2, the *Ro*PYC N315F/ R485P/N1078F orf in pY15TEF1	This work
pY15TEF1-*Ro*PYC*	Amp, LEU2, the *Ro*PYC* orf in pY15TEF1	This work
pY15TEF1-*Ro*PYC* N315F	Amp, LEU2, the *Ro*PYC* N315F orf in pY15TEF1	This work
pY15TEF1-RoPYC* R485P	Amp, LEU2, the *Ro*PYC* R485P orf in pY15TEF1	This work
pY15TEF1-RoPYC* N1078F	Amp, LEU2, the *Ro*PYC* N1078F orf in pY15TEF1	This work
pY15TEF1-RoPYC* N315F/R485P	Amp, LEU2, the *Ro*PYC* N315F/ R485P orf in pY15TEF1	This work
pY15TEF1-RoPYC* R485P/N1078F	Amp, LEU2, the *Ro*PYC* R485P/ N1078F orf in pY15TEF1	This work
pY15TEF1-RoPYC* N315F/N1078F	Amp, LEU2, the *Ro*PYC* N315F/ N1078F in pY15TEF1	This work
pY15TEF1-RoPYC* N315F/R485P/ N1078F	Amp, LEU2, the *Ro*PYC*N315F/ R485P/N1078F orf in pY15TEF1	This work

Industrial-scale and safety restriction of fumaric acid production by *Rhizopus oryzae* limit its wide usage; on the other hand, *S. cerevisiae* is safe and genetically tractable, allowing for the successful construction of a synthetic pathway of fumaric acid in this organism. Our previous work has demonstrated that overexpression of *Ro*PYC can significant improve fumaric acid production, and we were the first to report that the mutation P474N[Pro→Asn] in *Ro*PYC leads to a 13.3% increase of PYC activity and a 24.8% increase in fumaric acid titer [10]. Subsequently, we would like to conduct site-saturation mutagenesis for further improving fumaric acid production, and for this reason we wanted to identify more target sites for mutation in *Ro*PYC. It was reported that these residues (Lys^{245}, Glu^{283}, Glu^{297}, and Asn^{299}) were important for interacting with ATP, whereas the residues Arg^{472} created strong interaction with 5′ α-phosphate of ethyl-CoA, based on the analysis of the crystal structure of PYC from *Rhizobium etli* (*Re*PYC) [11]. In addition, it was also reported that the peptide (from Asp^{1018} to Asp^{1065}) including Asn^{1055} linked the CT domain and the biotin carboxyl carrier protein domain [11].

Considering that PYC is conserved, protein sequences alignment between *Re*PYC and *Ro*PYC shows that these residues (Lys^{245}, Glu^{283}, Glu^{297}, Asn^{299}, Arg^{472} and Asn^{1055}) in *Re*PYC and the corresponding residues (Lys^{262}, Glu^{300}, Glu^{313}, Asn^{315}, Arg^{485}, and Asn^{1078}) in *Ro*PYC are conserved (Fig. S1). Thus, engineering these key residues may provide mutants that can lead to higher fumaric acid production in *S. cerevisiae*. Meanwhile, the high prevalence of rare codons, is known to negatively influence translational efficiency [12]. The translational efficiency of heterologous genes can be improved by optimizing synonymous codon usage to better match the translation system in a specific host strain [13,14].

In addition, calcium ion (Ca^{2+}) is involved in cellular signaling pathways [15,16] and influences pyruvate carboxylase activity [17].

Table 2
Production of fumaric acid in the engineered strains expressing the wildtype *Ro*PYC and the mutants at 96 h of fermentation.

PYC	Titer of fumaric acid (mg/L)
Wild-type	238 ± 11.4
E300C	248 ± 9.8
N315F	290 ± 11.2
R485P	312 ± 14.0
N1078F	309 ± 12.0
N315F/ R485P	210 ± 9.6
R485P/N1078F	215 ± 10.4
N315F/N1078F	218 ± 10.2
N315F/ R485P/ N1078F	212 ± 9.2

Each value represents the mean and standard deviation of three independent measurements.

Addition of $CaCl_2$ can increase malate yield [18]. Furthermore, carbon dioxide (CO_2) is the substrate of pyruvate carboxylase in the carboxylation of pyruvate (a C_3 carbon molecule) to oxaloacetate (C_4 carbon), and the positive effects of CO_2 on malate [18] and succinate [19] production have also been observed. The combined effect of calcium and CO_2 on PYC activity and fumaric acid production remains unknown.

In this work, we semi-rationally evolved *Ro*PYC by site-saturation mutagenesis and codon optimization to improve fumaric acid production in *S. cerevisiae*. Firstly, we selected Lys^{262}, Glu^{300}, Glu^{313}, Asp^{315}, Arg^{485}, and Asp^{1078} in *Ro*PYC as the targets for site-saturation mutagenesis. We then optimized the codon of *RoPYC* and conducted site-directed mutagenesis in codon-optimized *Ro*PYC to further improve fumaric acid production. Subsequently, enzyme assays of PYC and its mutants as well as their structural modeling were performed. Finally, we investigated the effect of Ca^{2+} and CO_2 on fumaric acid production in *S. cerevisiae*.

2. Materials and methods

2.1. Strains, plasmids, media, and fermentation condition

All strains and plasmids used in this study are listed in Table 1. The Cre-expressing plasmid pSH47 was used for marker rescue.

Yeast extract peptone dextrose (YPD) medium, containing 10 g/L yeast extract, 20 g/L peptone, and 20 g/L glucose, was used for seed culture. Fermentation was performed in synthetic dextrose (SD) medium, containing 40 g/L glucose, 3.4 g/L yeast nitrogen base, 5 g/L ammonium sulfate, and mixed amino acids of 100 mg/L uracil, 100 mg/L leucine, 20 mg/L histidine and 40 mg/L tryptophan. The medium was sterilized for 20 min at 115 °C and sterilized $CaCO_3$ was added to the medium at a final concentration of 5 g/L. The seed culture was prepared by inoculating a single colony from YPD plate into a 100-mL flask containing 50 mL of YPD medium and incubating overnight. Then, the overnight culture was inoculated into a 250-mL flask containing 40 mL of SD medium at a final OD_{600} of 0.2, and aerobic fermentation was

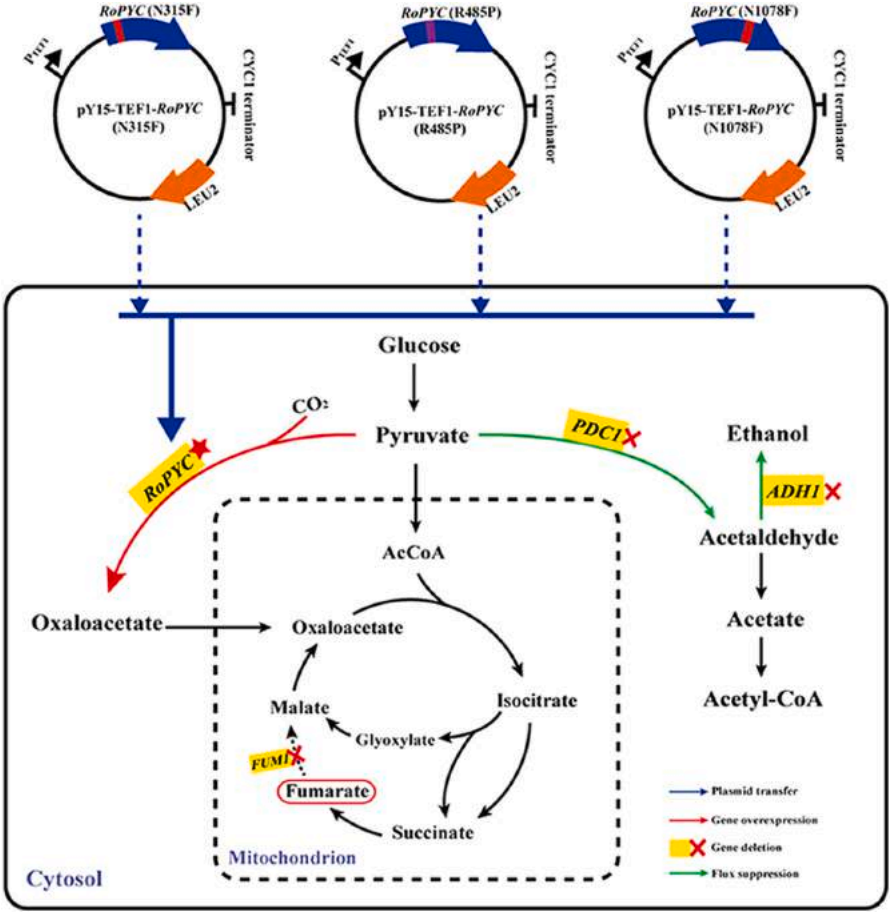

Fig. 1. Major metabolic pathway leading to fumaric acid formation in *S. cerevisiae*. Abbreviations of enzymes: pyruvate carboxylase (PYC), pyruvate decarboxylase (PDC1), alcohol dehydrogenase (ADH1), fumarase (FUM1). Green full line indicate reduced enzyme activity due to gene deletion, dotted line with X mark indicates missing enzyme activity due to gene deletion, red full line indicates enhanced enzyme activity due to gene overexpression.

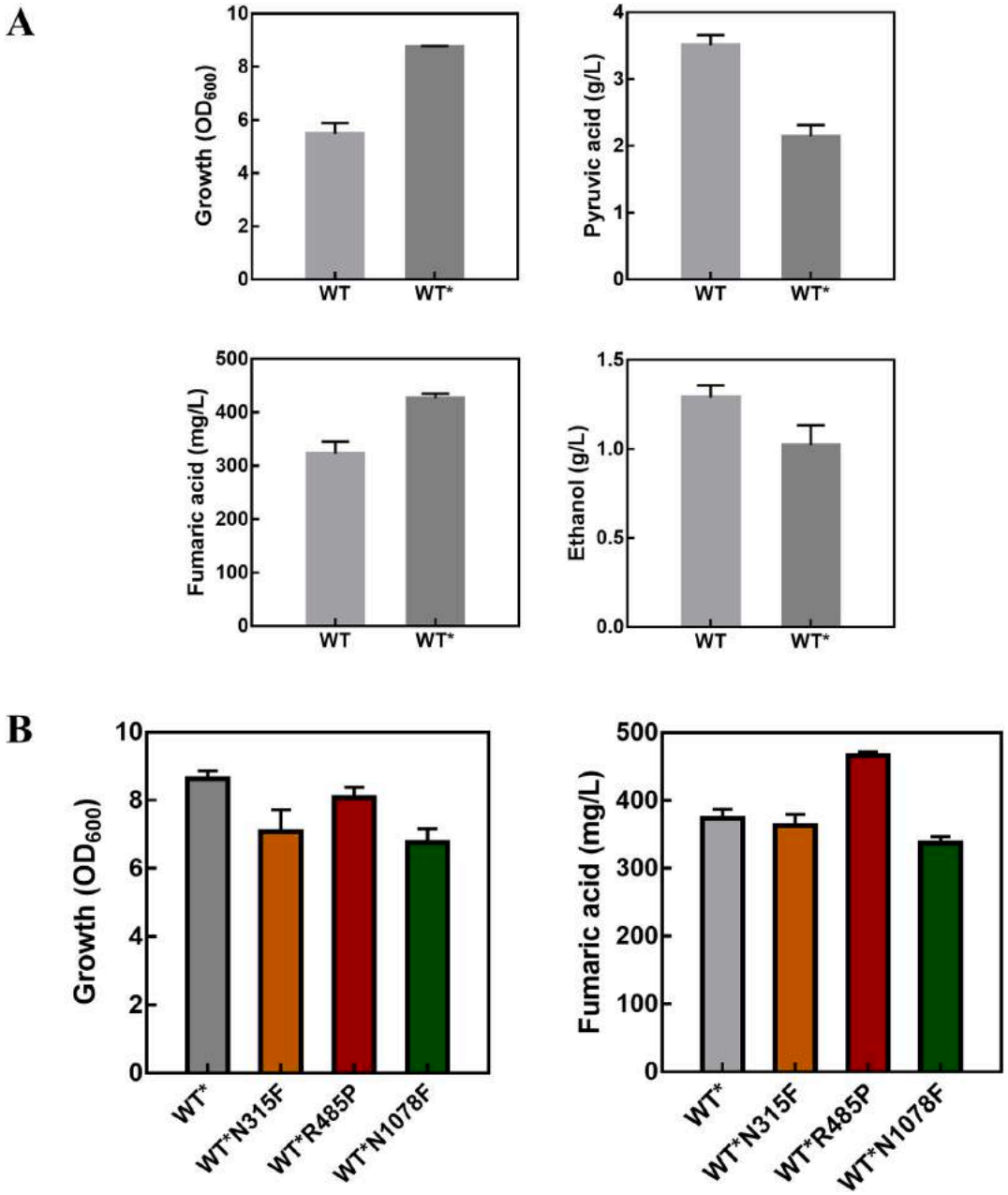

Fig. 2. Directed evolution in codon-optimized *RoPYC* to enhance fumaric acid production. **(A)** Effect of codon optimization of pyruvate carboxylase gene on fumaric acid fermentation (cell growth, fumaric acid production, pyruvate and ethanol production). WT represents the engineered strain *pdc1adh1fum1* with wild type *RoPYC*, and WT* represents the engineered strain *pdc1adh1fum1* with codon optimized *RoPYC*. Values represent the average and standard deviations of three independent experiments. **(B)** Effect of site-directed mutagenesis in optimized codon of pyruvate carboxylase on fumaric acid fermentation (cell growth and fumaric acid). The strains contain engineered strain *pdc1adh1fum1* with codon *RoPYC**, the engineered strain with the mutant *Ro*PYC*N315F, the engineered strain with the mutant *Ro*PYC*R485P, and the engineered strain with the mutant *Ro*PYC*N1078F. Values represent the average and standard deviations of three independent experiments.

conducted at 30 °C under constant shaking (220 rpm).

For each bioreactor experiment, batch culture processes were performed in a 7-L bioreactor (Bioflow110; New Brunswick Scientific Co., Edison, NJ, USA) containing 4-L SD medium with 40 g/L glucose at 30 °C. 25 mM $CaCl_2$ was added into the medium. pH was controlled at 4.8 by automatically feeding 2 M KOH during the fermentation process. For CO_2-sparging fermentation, pure CO_2 was mixed with air at a ratio (v/v) of 1:10. The dissolved oxygen concentration was maintained at 10% by auto-regulating agitation and air. Antifoam (Sigma 204) was added to control foaming.

2.2. Site saturation mutagenesis and transformation

For saturation mutagenesis, PCR was performed with Prime STAR GXL DNA polymerase (TaKaRa Bio, Co., Ltd., Dalian, China) using the plasmid pY15TEF1-RoPYC as the template. The oligonucleotides used

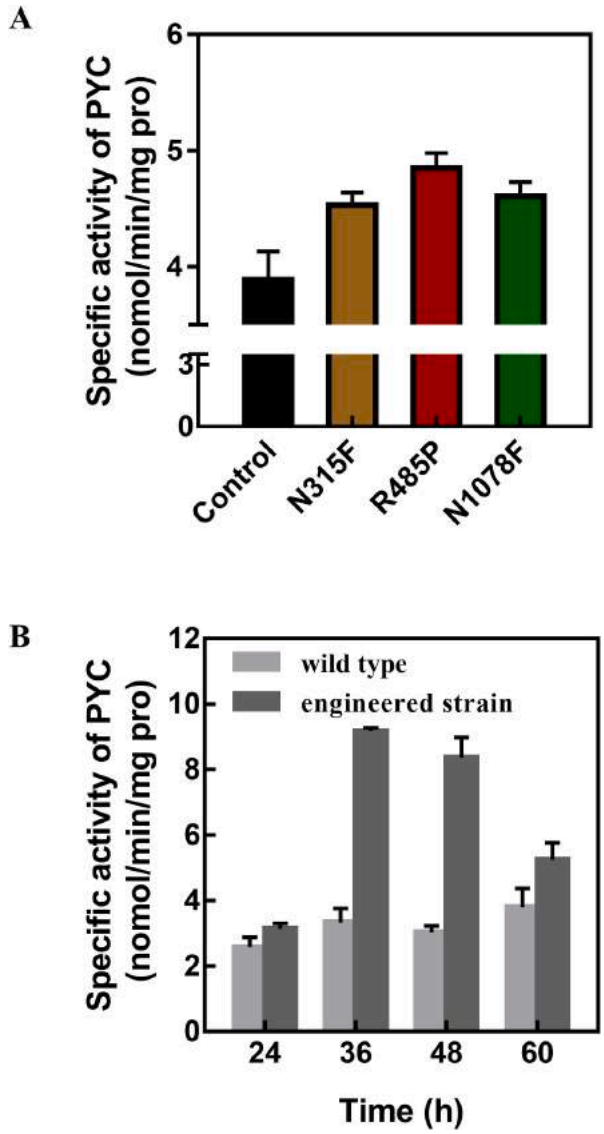

Fig. 3. The enzymatic activity of *Ro*PYC and its mutants in engineered strain *pdc1adh1fum1*. **(A)** Comparing enzymatic activity between *Ro*PYC and its mutants N315F, R485P and N1078F, **(B)** The PYC activity of the engineered stain *pdc1adh1fum1↑RoPYC*R485P* at different time-points (24 h, 36 h, 48 h and 60 h).

for site-saturation mutagenesis of Lys262, Glu300, Glu313, Asp315, Arg485, and Asn1078 are listed in Table S1. The underlined nucleotides (corresponding to Lys262, Glu300, Asp315, Arg485, and Asn1078) were replaced with the following codons: phenylalanine (ttt), leucine (ttg), isoleucine (att), methionine (atg), valine (gtt), serine (tct), proline (cca), threonine (act), alanine (gct), tyrosine (tat), histidine (cat), glutamine (caa), lysine (aaa), aspartic acid (aat), glutamic acid (gaa), cysteine (tgt), tryptophan (tgg), arginine (aga), glycine (ggt), and asparagine (ggt). For the construction of double and triple mutants, the product of the first PCR mutagenesis was used as the template for the subsequent PCR. Then, all of the PCR products were treated with QuickCutTM *Dpn*I enzyme (TaKaRa Bio, Co., Ltd., Dalian, China) before being transformed into *Escherichia coli* Trans1-T1Phage Resistant cells. Correct constructs were confirmed by DNA sequencing. The correct plasmids were transformed into *S. cerevisiae* CEN.PK2–1 C *pdc1adh1fum1* cells using a Frozen-EZ Yeast Transformation II kit (Zymo Research, Orange, CA, USA), according to the recommended protocol.

2.3. Codon optimization of RoPYC and site directed mutagenesis

The codons of the *Ro*PYC gene (3540 bp, GenBank Accession No. HM130700.1) were optimized based on the codon preference of *S. cerevisiae* using a codon adaptation tool (http://www.jcat.de/). The DNA sequence was optimized for protein overexpression in *S. cerevisiae* without altering the encoded amino acid sequence. The codon-optimized *Ro*PYC (*Ro*PYC*) (3540 bp, GenBank Accession No. BankIt2458471 Seq1 MZ227581) was artificially synthesized by Shanghai Sangong Co., Ltd (Shanghai, China). For site-directed mutagenesis, PCR was performed with Prime STAR GXL DNA polymerase (TaKaRa Bio, Co., Ltd., Dalian, China) using the plasmid pY15TEF1-RoPYC* as the template DNA. The oligonucleotides used for site-saturation mutagenesis of Asp315, Arg485, and Asn1078 are listed in Table S2. The underlined nucleotides (corresponding to Asp315, Arg485, and Asn1078) were replaced with the following codons: phenylalanine (ttt), proline (cca) and phenylalanine (ttt), respectively. The remaining steps are the same as described in the section "Site saturation mutagenesis".

2.4. Structural modeling

*Ro*PYC structure including carboxyltransferase domain, central allosteric domain, and biotin carboxylation domain was predicted by molecular modelling through the online software, Swissmodel (http://swissmodel.Expasy.org/). Other tools included Deepview V4.1 and Pymol. *Ro*PYC RNA has been translated into protein sequence Expasy translate tool. (https://web.expasy.org/translate/). *Ro*PYC protein sequence was used as the target sequence to search for a template library. About 50 PDB templates were found. Template (3bg5), which has the same substrate (PYRUVIC ACID) in carboxyltransferase domain was selected as the template for homology modelling (coverage 97% and identity 49.9%) to build catalytic domain. Template (2qf7), (coverage 97% and identity 49.5%) which has the same coenzyme A binding sites in the allosteric domain was selected as the modeling template to construct allosteric domain. Both models have good quality with GMQE (Global Model Quality Estimation) valued at 0.73. The predicted structure models were later subjected to energy minimization using Deepview V4.1.

2.5. Enzyme activity assays

Cells at different stages were harvested by centrifugation at 6120 *g* for 1 min at 4 °C. The cells were then used to extract total crude enzymes as described elsewhere [20]. The protein concentration was determined using bovine serum albumin as standard as described in a previous study [21]. The PYC activity was measured as described elsewhere [22]. The reaction mixture (1 mL) contained 100 μmol Tris buffer (pH 7.8), 0.1 μmol acetyl-CoA, 20 μmol $KHCO_3$, 7.5 μmol $MgSO_4$, 10 μmol potassium pyruvate, 0.15 μmol NADH, 12 U malate dehydrogenase (Sigma), and cell-free extract. The reaction was started with the addition of 4 μmol ATP, and the PYC activity was measured at 340 nm. One unit of enzyme activity was defined as consumption of 1 nM NADH per minute per gram of fresh cell.

2.6. Biomass and metabolite determination

To dissolve residual $CaCO_3$, each culture broth was diluted to an appropriate concentration with 0.1 M HCl for OD measurement at 600 nm on a spectrophotometer. Extracellular concentrations of pyruvate, ethanol, and glucose were determined by high-performance liquid chromatography (HPLC) using a Bio-Rad Aminex HPX-87H column (Bio-Rad, Hercules, CA, USA) eluted with 5 mM H_2SO_4 at a flow rate of 0.6

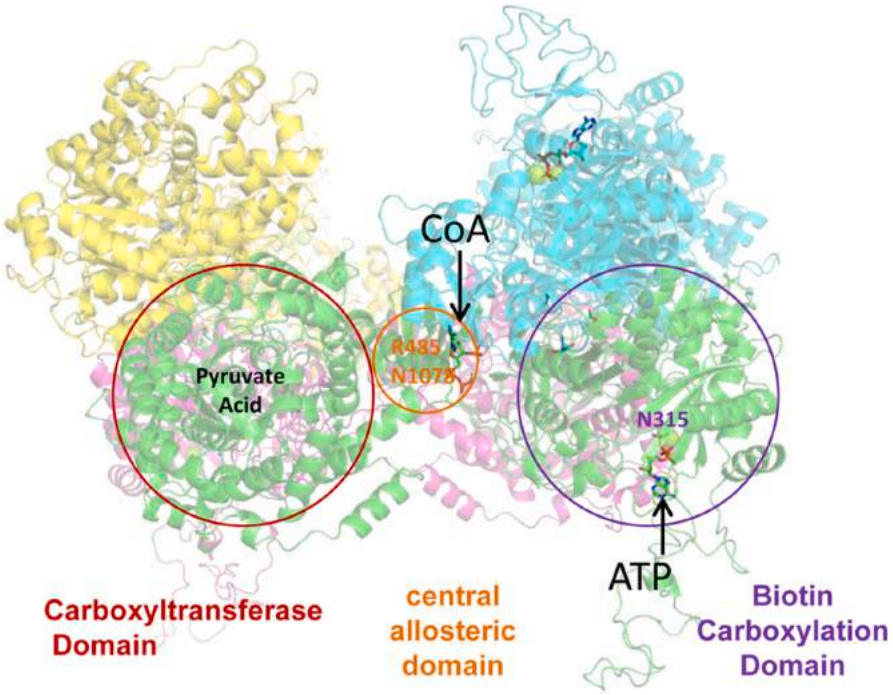

Fig. 4. The new *Ro*PYC model contains an asymmetric tetramer (different colors represent different chains). Monomer A (green ribbon) consists of Carboxyltransferase Domain (red circle), central allosteric domain (orange circle) and Biotin Carboxylation Domain (purple circle). R485 and N1078 are located in the central allosteric domain close to CoA, while N315 is located in the Biotin Carboxylation Domain, close to ATP.

mL/min at 35 °C. Ethanol and glucose were detected with a Waters 2410 refractive index detector (Waters, Milford, MA, USA), while pyruvate and fumaric acid were detected using a Waters 2489 series VWD at 210 nm. The data was presented as average and standard deviation of three independent experiments.

3. Results

3.1. Alteration of key residues in RoPYC for elevating fumaric acid production

Previously, in order to reduce the carbon flux toward ethanol from pyruvate, we deleted the pyruvate decarboxylase (PDC1) which can result in 30% decrease in pyruvate decarboxylase activity without affecting the maximum growth rate, and deleted the major enzyme ethanol dehydrogenase (ADH1) responsible for the production of ethanol from acetaldehyde by deleting *PDC1* and *ADH1* in the *S. cerevisiae* cells, which led to a 42.7% decrease in the maximum titer of ethanol compared with the wild-type cells. Subsequently, we constructed a synthetic pathway of fumaric acid by deleting *FUM1* in the *pdc1adh1* strain, which led to accumulation of 194.0 ± 4.0 mg/L fumaric acid [10]. Based on this study, we overexpressed the heterologous *Ro*PYC gene in the *pdc1adh1fum1* strain. Protein sequence alignment between *Ro*PYC and *Re*PYC, whose crystal structure is available, showed that the residues (Lys^{262}, Glu^{300}, Glu^{313}, Asn^{315}, Arg^{485}, and Asn^{1078}) are potential active residues. Thus, site-saturation mutagenesis of the selected six sites was performed in *Ro*PYC to further elevate fumaric acid production. Among all the *Ro*PYC mutants examined, only N315F, R485P, and N1078F mutants produced higher yields of fumaric acid (290 ± 11.2, 312 ± 14.0, and 309 ± 12.0 mg/L, respectively), which were 22.0%, 31.1%, and 29.9% higher than that produced by the wild-type *Ro*PYC (238 ± 11.4 mg/L), respectively (Table 2), while other mutants produced lower yields of fumaric acid (Table S3). In contrast, mutagenesis of Lys^{262}, Glu^{300}, or Glu^{313} led to a dramatic decrease in fumaric acid production, except E300C that showed a slight increase in fumaric acid production (Table 2). Based on these results, to further enhance fumaric acid production, we constructed double and triple mutants, namely, N315F/R485P, R485P/N1078F, N315F/N1078F, and N315F/R485P/N1078F. However, overexpression of each of these mutants slightly decreased fumaric acid production, when compared with that produced by the wild-type *Ro*PYC in the *pdc1adh1fum1* strain (Table 2). Fig. 1.

3.2. Codon-optimization of RoPYC leads to fumaric acid production improvement

Analysis of the wild-type *RoPYC* revealed that some of its codons are rare in *S. cerevisiae*. Therefore, we hypothesized that codon optimization of *RoPYC* might be able to increase its protein expression in *S. cerevisiae.* Two strains overexpressing wild-type *RoPYC* and codon-optimized *RoPYC** were compared. As shown in Fig. 2A, overexpression of codon-optimized *RoPYC** increased the maximal biomass to OD_{600} of 8.75 ± 0.04 and the maximal fumaric acid titer to 426.4 ± 8.9 mg/L at 96 h, which were 59.7% and 32.2% higher than those produced by the wild-type *RoPYC* (OD_{600} = 5.48 ± 0.40 and fumaric acid titer = 322.6 ± 22.6 mg/L), respectively. Meanwhile, overexpression of codon-optimized *RoPYC** produced pyruvate and ethanol at 2.14 ± 0.17 mg/L and 0.83 ± 0.19 g/L, which were 39.0% and 48.1% lower than those produced by the wild-type *RoPYC* (3.51 ± 0.15 mg/L and 1.60 ± 0.12 g/L), respectively.

3.3. Engineering of codon-optimized RoPYC to enhance fumaric acid production

As demonstrated earlier, both site-directed mutagenesis of *Ro*PYC (N315F, R485P, and N1078F) and codon optimization had a positive impact on the production of fumaric acid. We subsequently constructed three codon-optimized *Ro*PYC* mutants (N315F, R485P, and N1078F)

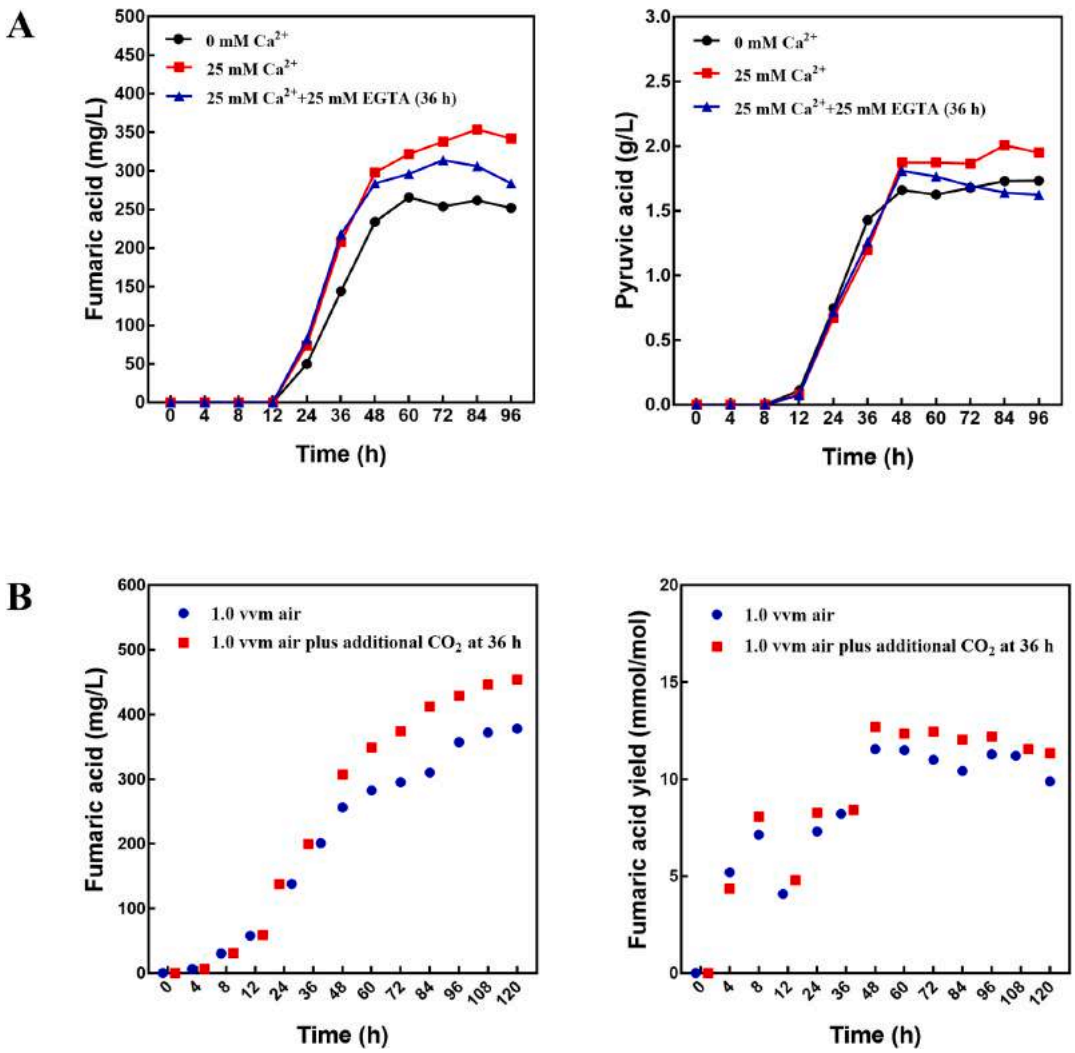

Fig. 5. Effect of calcium ion or CO_2 on fumaric acid fermentation of the engineered strain *pdc1adh1fum1*↑*RoPYC**R485P. **(A)** Effect of calcium ion on the titer of fumaric acid and pyruvic acid production. Circles represent the fermentation without the addition of calcium ion; squares represent the fermentation with addition of 25 mM calcium ion at the beginning; triangles represent the fermentation with addition of 25 mM calcium ion at the beginning, and then 25 mM EGTA at 36 h. **(B)** Effect of CO_2 on the titer of fumaric acid and the yield of fumaric acid from glucose. Squares represent the fermentation sparged with 1 vvm air in the whole stage; circles represent the fermentation sparged with 1 vvm air in the stage (0–36 h), then with additional 0.1 vvm CO_2 until 120 h.

and overexpressed them in the *pdc1adh1fum1* strain. As shown in Fig. 2B, overexpression of *RoPYC*N315F*, *RoPYC*R485P,* or *RoPYC*N1078F* caused slightly lower maximal biomass, when compared with that of the codon-optimized *RoPYC**. Overexpression of *RoPYC*R485P* resulted in a maximal fumaric acid titer of 465.5 ± 6.5 mg/L at 120 h, which was 24.6% higher than that produced by the codon-optimized *RoPYC** at 108 h (373.5 ± 13.4 mg/L); however, overexpression of *RoPYC*N315F* and *RoPYC*N1078F* caused a 7.0% and 10.9% decrease in the maximal fumaric acid titers at 108 h, respectively, when compared with that produced by the codon-optimized *RoPYC** (Fig. 2B). Accordingly, we further constructed three double mutants, N315F/R485P, R485P/N1078F, and N315F/N1078F PYC* and the triple mutant N315F/R485P/N1078F PYC*, and investigated their effects on fumaric acid production. Like the corresponding non-codon-optimized PYC, the fumaric acid titers produced by the engineered strains overexpressing these mutants were almost the same as that produced by the codon-optimized *RoPYC** (data not shown). Therefore, the mutant *RoPYC*R485P* was chosen for further examination.

3.4. Enzyme assay and structural modeling of pyruvate carboxylase and its mutants

The enzymatic activities of *Ro*PYC and its mutants in the engineered yeast strains were determined. As shown in Fig. 3A, the mutants N315F, R485P, and N1078F displayed higher enzymatic activities than the wild type *Ro*PYC, and the activity of the mutant R485P was the highest among the three, which was consistent with the performance in fumaric acid production. Furthermore, PYC activities of the mutant R485P and the wild type strain were accessed across the whole fermentation process, as shown in Fig. 3B. The mutant strain R485P showed higher activities than the wild type throughout the fermentation with the maximum activity up to 9.18 ± 0.10 U at 36 h, which was 175.3% higher than the highest activity in the wild type strain CEN.PK2–1C. The increased PYC activity could directly explain why fumaric acid titer increased up to 465.5 ± 6.5 mg/L from 194.0 ± 4.0 mg/L.

In order to elucidate the behavior of the mutants on the molecular level, the molecular modeling of *Ro*PYC and its mutants was performed. To investigate the activation site, a model was built based on the crystal

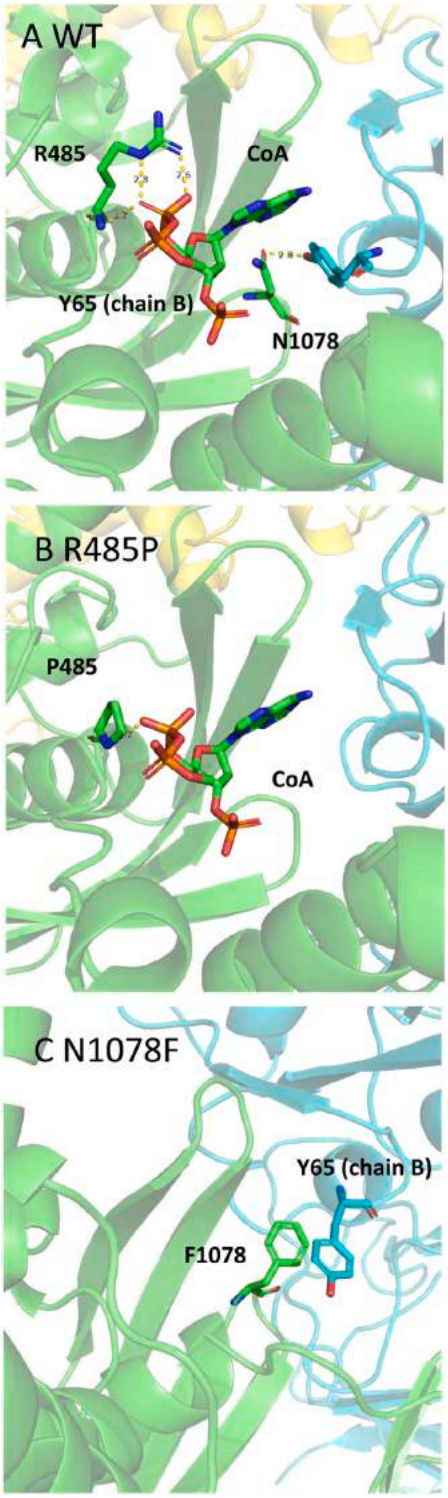

Fig. 6. (A) In wild type, interaction of R485 and N1078 in central allosteric domain. R485 of the allosteric domain formed triple H-bonds with phosphate of ethyl-CoA. N1078 formed intermolecular H-bond with Y65 from chain B. **(B)** Mutant R485P only form 1 possible H-Bond with CoA. **(C)** Mutant N1078F could not form inter-chain H-bond with Y65 or any other residues from chain B. Labeled H-bond distance is from center of donor to center of receptor. For example: in the N-H···O═C bond, it is the N-O distance.

structure of *Staphylococcus aureus* pyruvate carboxylase (PDB ID 3bg5) [23], which has the same substrate (pyruvate acid). Models showed that WT and mutants have nearly the same structure of catalytic pocket (RMSD<0.01), which indicated that the increase of fumaric acids are not caused by modulation in the catalytic pocket (Fig. 4). Then allosteric domain was investigated, and model was built based on the structure of a complete multifunctional pyruvate carboxylase from *Rhizobium etli* (PDB ID 2qf7) [11], which has Coenzyme A binding sites in the allosteric domain. Interestingly, models showed that WT and mutants have very different CoA binding pockets, which indicated that increasing the allosteric domain flexibility might further increase activity of whole enzyme (Fig. 4). As shown in Fig. 4, R485 and N1078 are located in the central allosteric domain close to CoA, while N315 is located in the biotin carboxylation domain, close to ATP.

3.5. Positive impact of calcium ion and carbon dioxide on fumaric acid production in 7-L bioreactor

We next investigated fumaric acid fermentation in a 7-L bioreactor to monitor the possible impact of calcium ion (Ca^{2+}) on fumaric acid production by the mutant *Ro*PYC**R485P*. Different concentrations of Ca^{2+} (0 mM, 5 mM, 25 mM and 125 mM) were fed into bioreactor batch cultures grown at pH 4.8. It was shown that 25 mM Ca^{2+} led to maximal fumaric acid production (Fig. S2). Then the role of Ca^{2+} in fumaric acid fermentation was confirmed by removing Ca^{2+} through the addition of EGTA. Addition of 25 mM EGTA at 36 h decreased the fumaric acid titer and concurrently caused 16.0% more accumulation of pyruvate (Fig. 5A).

It is known that CO_2 plays a critical role as a substrate of pyruvate carboxylase in pyruvate carboxylation. Supplementation of CO_2 has been shown to improve the production of both malate and succinate [18]. Therefore, we examined whether CO_2 supplementation would have a positive impact on fumaric acid production by sparging 10% additional CO_2 into the 7-L bioreactor as well as 1.0 vvm air. When CO_2 was inflated from 36 h (early stationary phase), the fumaric acid titer increased, reaching 453.6 mg/L, which was 20% higher than that observed in the control (378 mg/L) (Fig. 5B). Moreover, the CO_2 supply increased fumaric acid yield on glucose (Fig. 5B), and the maximum yield was 11.34 mg/g, which was 14.8% higher than that in the control.

4. Discussion

Pyruvate carboxylase (PYC) is a limiting step in the production of dicarboxylic acids in microbial fermentation processes. Heterologous overexpression of pyruvate carboxylase gene from *Rhizopus oryzae* resulted in limited improvement of fumaric acid titer. To further elevate fumaric acid production in the engineered yeast strain, semi-rational evolution of pyruvate carboxylase might be beneficial. For this reason, we performed protein engineering of *Ro*PYC by using site-saturation mutagenesis, and successfully generated three mutants (PYC) with enhanced enzyme activities, which led to a dramatic increase in fumaric acid production.

Interestingly, among all the mutants, the N315F, R485P, and N1078F mutants produced the highest fumaric acid yields. Homology modeling indicated that the increased PYC activities could be attributed to the modulation of the allosteric domain and the biotin carboxylation domain. However, the exact mechanism for that has yet to be elucidated (Fig. 4). Residue R485 in the allosteric domain formed triple H-bonds with phosphate of acetyl-CoA (Fig. 6A) while mutation R485P formed only one possible H-bond (Fig. 6B). N1078 formed intermolecular H-bond with Y65 from the same chain (Fig. 6A), while mutant R485P only formed one possible H-bond with CoA (Fig. 6B), but the mutant N1078F could not form inter-chain H-bond with Y65 or any other residues from another monomer chain B (Fig. 6C). These two mutations (R485P, and N1078F) can increase the flexibility of allosteric domain and thereby increase total enzymatic activity (Figs. 3A and B). We further compared

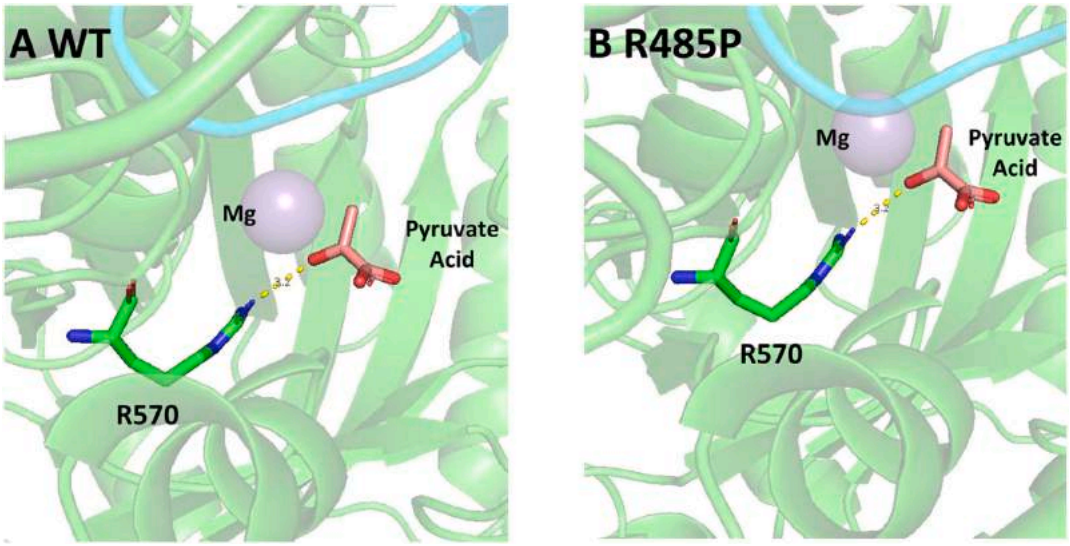

Fig. 7. Compare Carboxyltransferase Domain between A) wild type and B) R485P. One H-bond formed between pyruvate acid and R570, and the distance is 3.2 A in both models. The structures of both models are highly similar with RMSD< 0.01.

carboxyltransferase domains between the wild type PYC and the mutant R485P and observed that one H-bond formed between pyruvate acid and R570 with the distance of 3.2 A in both models, which means that the structures of both models are highly similar with RMSD< 0.01 (Fig. 7A and B). In addition, N315 is close to the ATP binding site in the biotin carboxylation domain. When N315 mutates to F315, the newly formed aromatic ring may help with better ATP binding/turnover (Fig. S3). Allosteric regulation alters carrier domain translocation in pyruvate carboxylase [24]. A distinct holoenzyme organization for two-subunit pyruvate carboxylase [25].

Unexpectedly, unlike previous reports that double or triple mutants perform better than single mutants [26], they did not lead to a higher fumaric acid titer in this work. A possible explanation for this could be that the hydrophobic amino acids (phenylalanine and proline) removed all the possible hydrogen-binding interactions between the amino residue and substrate, thus affecting the stability of the bent conformation. In protein structure, one mutation has limited negative effect on protein stability because stability surplus could buffer its destabilizing effect. However, the buildup of multiple mutations might lead to a dramatic reduction in stability which could lead to activity decline [27,28]. In the double mutant of R485/N1078F, the single mutation at R485P or N1078F might bring a higher flexibility of the allosteric domain to facilitate better active-site pairing, which could bring a better yield. However, double mutations might cause a severe loss of linkage stability in the allosteric domain and therefore could lead to a decrease in yield.

In addition, Ca^{2+} addition demonstrated positive effect on fumaric acid production, which is consistent with previous studies that a modest increase in malate yield was observed when 5 or 10 mM $CaCl_2$ was added [18] and that succinic acid production was increased by adding $CaCO_3$ [29]. A possible explanation for this could be that Ca^{2+} is known to be involved in cellular signaling pathways [15,16] and to influence pyruvate carboxylase activity [17], while the exact mechanism for that has yet to be elucidated. Furthermore, supplementing CO_2 can also increase fumaric acid titer and yield. It has also been shown that C_4 dicarboxylic acid production can benefit from the supply of CO_2 by bacterium *Mannheimia succiniciproducens* [30], *Escherichia coli* [31,32] or by yeast *S. cerevisiae* [18,33]. This positive effect can be explained by more favorable kinetics or thermodynamics of the carboxylation reactions in C_4 dicarboxylic acid production.

In summary, semi-rational evolution of pyruvate carboxylase from *Rhizopus oryzae* is effective for elevating fumaric acid synthesis in *S. cerevisiae*. This represents a promising approach for enhancing metabolic flow to the target compound by evolution of the key enzyme, and demonstrated a useful way for further enhancing the synthesis of dicarboxylic acids.

Funding information

We thank Prof. Liming Liu for his support regarding this project and Prof. Linghuo Jiang for his helpful suggestion on the manuscript. This work was partially supported the National Key Research and Development of China Program (2020YFA0908300), National Natural Science Foundation of China (No. 31300027 and No. 81371784), Jiangsu Provincial Natural Science Foundation (No. BK20130136 and No. BK20191333), national first-class discipline program of Light Industry Technology and Engineering (LITE2018–11), the Open Project Program for Key Laboratory of Fermentation Engineering (Ministry of Education) (No. KLIB-KF201606), Program of Introducing Talents of Discipline to Universities (No. 111-2-06), and China Postdoctoral Science Foundation (No. 2014M550266). International Joint Research Laboratory for Engineering Synthetic Biosystem for Intelligent Biomanufacturing at Jiangnan University.

Ethical approval

This article does not contain any studies with human participants or animals performed by any of the authors.

CRediT authorship contribution statement

XG conceived and designed research. SX, GY, WJ, CH, LY, CY, LJ and XX conducted experiments. XG and XK analyzed the data. XG wrote the manuscript. ZJ, LR, ZX and SJ contributed with scientific discussions and commented on the manuscript. XG, KM and XZ supervised the work and revised the manuscript. All authors read and approved the manuscript.

Author contributions

XG conceived and designed research. SX, GY, WJ, CH, LY, CY, LJ and XX conducted experiments. XG and XK analyzed the data. XG wrote the manuscript. ZJ, LR, ZX and SJ contributed with scientific discussions

and commented on the manuscript. XG, KM and XZ supervised the work and revised the manuscript. All authors read and approved the manuscript.

Declaration of Competing Interest

The authors declare that they have no known competing financial interests or personal relationships that could have appeared to influence the work reported in this paper.

Data availability

The datasets generated during and/or analyzed during the current study are available from the corresponding author on reasonable request.

Appendix A. Supporting information

Supplementary data associated with this article can be found in the online version at doi:10.1016/j.bej.2021.108238.

References

[1] Z. Dai, H. Zhou, S. Zhang, H. Gu, Q. Yang, W. Zhang, W. Dong, J. Ma, Y. Fang, M. Jiang, F. Xin, Current advance in biological production of malic acid using wild type and metabolic engineered strains, Bioresour. Technol. 258 (2018) 345–353.

[2] M. Jiang, J. Ma, M. Wu, R. Liu, W. Dong, Progress of succinic acid production from renewable resources: metabolic and fermentative strategies, Bioresour. Technol. 245 (2017) 1710–1717.

[3] M. Sauer, D. Porro, D. Mattanovich, P. Branduardi, Microbial production of organic acids: expanding the markets, Trends Biotechnol. 26 (2008) 100–108.

[4] X. Yin, J. Li, H. Shin, G. Du, L. Liu, J. Chen, Metabolic engineering in the biotechnological production of organic acids in the tricarboxylic acid cycle of microorganisms: advances and prospects, Biotechnol. Adv. 33 (2015) 830–841.

[5] G. Xu, L. Liu, J. Chen, Reconstruction of cytosolic fumaric acid biosynthetic pathways in *Saccharomyces cerevisiae*, Micro Cell Fact. 11 (2012) 24.

[6] D. Abbott, R. Zelle, J. Pronk, M. Van, Metabolic engineering of *Saccharomyces cerevisiae* for production of carboxylic acids: current status and challenges, FEMS Yeast Res. (2010) 1123–1136.

[7] S. Jitrapakdee, M. Maurice, I. Rayment, W. Cleland, Structure, mechanism and regulation of pyruvate carboxylase, Biochem. J. 413 (2008) 369–387.

[8] G. Xu, X. Chen, L. Liu, L. Jiang, Fumaric acid production in *Saccharomyces cerevisiae* by simultaneous use of oxidative and reductive routes, Bioresour. Technol. 148 (2013) 91–96.

[9] G. Xu, W. Zou, X. Chen, N. Xu, L. Liu, J. Chen, Fumaric acid production in *Saccharomyces cerevisiae* by in silico aided metabolic engineering, PLoS One 7 (2012) 52086.

[10] G. Xu, M. Wu, L. Jiang, Site-saturation engineering of proline 474 in pyruvate carboxylase from *Rhizopus oryzae* to elevate fumaric acid production in engineered *Saccharomyces cerevisiae* cells, Biochem. Eng. J. 117 (2017) 36–42.

[11] M. Maurice, L. Reinhardt, K. Surinya, P. Attwood, J. Wallace, W. Cleland, I. Rayment, Domain architecture of pyruvate carboxylase, a biotin-dependent multifunctional enzyme, Science 317 (2007) 1076–1079.

[12] T. Tuller, Y. Waldman, M. Kupiec, E. Ruppin, Translation efficiency is determined by both codon bias and folding energy, Proc. Natl. Acad. Sci. U. S. A. 107 (2010) 3645–3650.

[13] A. Lanza, K. Curran, L. Rey, H. Alper, A condition-specific codon optimization approach for improved heterologous gene expression in *Saccharomyces cerevisiae*, BMC Syst. Biol. 8 (2014) 33.

[14] P. Zhou, L. Ye, W. Xie, X. Lv, H. Yu, Highly efficient biosynthesis of astaxanthin in *Saccharomyces cerevisiae* by integration and tuning of algal *crtZ* and *bkt*, Appl. Microbiol. Biotechnol. 99 (2015) 8419–8428.

[15] T. Matsumoto, A. Ellsmore, S. Cessna, P. Low, J. Pardo, R. Bressan, P. Hasegawa, An osmotically induced cytosolic Ca^{2+} transient activates calcineurin signaling to mediate ion homeostasis and salt tolerance of *Saccharomyces cerevisiae*, J. Biol. Chem. 277 (2002) 33075–33080.

[16] L. Viladevall, R. Serrano, A. Ruiz, G. Domenech, J. Giraldo, A. Barceló, J. Ariño, Characterization of the calcium-mediated response to alkaline stress in *Saccharomyces cerevisiae*, J. Biol. Chem. 279 (2004) 43614–43624.

[17] L. Liu, Y. Li, Y. Zhu, G. Du, J. Chen, Redistribution of carbon flux in *Torulopsis glabrata* by altering vitamin and calcium level, Metab. Eng. 9 (2007) 21–29.

[18] R. Zelle, E. Huister, W. Kloezen, J. Pronk, V. Maris, Key process conditions for production of C_4 dicarboxylic acids in bioreactor batch cultures of an engineered *Saccharomyces cerevisiae* strain, Appl. Environ. Microbiol. 76 (2010) 744–750.

[19] L. Zhu, L. Zhang, L. Wei, H. Li, Y. Tang, Collaborative regulation of CO_2 transport and fixation during succinate production in *Escherichia coli*, Sci. Rep. 5 (2015) 17321.

[20] R. Zelle, E. Hulster, W. Winden, P. Waard, C. Dijkema, A. Winkler, G. J-MA, J. Dijken, A. Maris, Malic acid production by *Saccharomyces cerevisiae*: engineering of pyruvate carboxylation, oxaloacetate reduction, and malate export, Appl. Environ. Microbiol. 74 (2008) 2766–2777.

[21] M. Bradford, A rapid and sensitive method for the quantitation of microgram quantities of protein utilizing the principle of protein-dye binding, Anal. Biochem. 72 (1976) 248–254.

[22] P. Jong-Gubbels, P. Vanrolleghem, S. Heijnen, J. Dijken, J. Pronk, Regulation of carbon metabolism in chemostat cultures of *Saccharomyces cerevisiae* grown on mixtures of glucose and ethanol, Yeast 11 (1995) 407–418.

[23] S. Xiang, L. Tong, Crystal structures of human and *Staphylococcus aureus* pyruvate carboxylase and molecular insights into the carboxyltransfer reaction, Nat. Struct. Mol. Biol. 15 (2008) 295–302.

[24] Y. Liu, M. Budelier, K. Stine, M. Maurice, Allosteric regulation alters carrier domain translocation in pyruvate carboxylase, Nat. Commun. 9 (2018) 1384.

[25] P. Choi, J. Jo, Y. Lin, M. Lin, C. Chou, L. Dietrich, L. Tong, A distinct holoenzyme organization for two-subunit pyruvate carboxylase, Nat. Commun. 7 (2016) 12713.

[26] G. Li, X. Fang, F. Su, Y. Chen, L. Xu, Y. Yan, Enhancing the thermostability of *rhizomucor miehei* lipase with a limited screening library by rational-design point mutations and disulfide bonds, Appl. Environ. Microbiol. 84 (2018).

[27] H. Huang, A. Horiuchi, J. Goldberg, P. Greengard, A. Nairn, Site-directed mutagenesis of amino acid residues of protein phosphatase 1 involved in catalysis and inhibitor binding, Proc. Natl. Acad. Sci. U. S. A. 94 (1997) 3530–3535.

[28] N. Tokuriki, C. Jackson, L. Afriat-Jurnou, K. Wyganowski, R. Tang, D. Tawfik, Diminishing returns and tradeoffs constrain the laboratory optimization of an enzyme, Nat. Commun. 3 (2012) 1257.

[29] A. Raab, G. Gebhardt, N. Bolotina, D. Weuster-Botz, C. Lang, Metabolic engineering of *Saccharomyces cerevisiae* for the biotechnological production of succinic acid, Metab. Eng. 12 (2010) 518–525.

[30] H. Song, J. Lee, S. Choi, J. You, W. Hong, S. Lee, Effects of dissolved CO_2 levels on the growth of *Mannheimia succiniciproducens* and succinic acid production, Biotechnol. Bioeng. 98 (2007) 1296–1304.

[31] H. Wu, Q. Li, Z. Li, Q. Ye, Succinic acid production and CO_2 fixation using a metabolically engineered *Escherichia coli* in a bioreactor equipped with a self-inducing agitator, Bioresour. Technol. 107 (2012) 376–384.

[32] J.H. Yu, L.W. Zhu, S.T. Xia, H.M. Li, Y.L. Tang, X.H. Liang, T. Chen, Y.J. Tang, Combinatorial optimization of CO_2 transport and fixation to improve succinate production by promoter engineering, Biotechnol. Bioeng. 113 (2016) 1531–1541.

[33] D. Yan, C. Wang, J. Zhou, Y. Liu, M. Yang, J. Xing, Construction of reductive pathway in *Saccharomyces cerevisiae* for effective succinic acid fermentation at low pH value, Bioresour. Technol. 156 (2014) 232–239.